Environmental Pollution 280 (2021) 116876

Contents lists available at ScienceDirect

Environmental Pollution

journal homepage: www.elsevier.com/locate/envpol

Biochemical potential evaluation and kinetic modeling of methane production from six agro-industrial wastewaters in mixed culture☆

Naassom Wagner Sales Morais [a], Milena Maciel Holanda Coelho [b], Amanda de Sousa e Silva [a], Francisco Schiavon Souza Silva [a], Tasso Jorge Tavares Ferreira [a], Erlon Lopes Pereira [a], André Bezerra dos Santos [a, *]

[a] Department of Hydraulic and Environmental Engineering, Federal University of Ceará, Fortaleza, Ceará, Brazil
[b] School of Chemistry, Federal University of Rio de Janeiro, Rio de Janeiro, Rio de Janeiro, Brazil

ARTICLE INFO

Article history:
Received 4 July 2020
Received in revised form
12 February 2021
Accepted 2 March 2021
Available online 9 March 2021

Keywords:
Biomethanization
Anaerobic digestion
Renewable energy
Agro-industrial wastewater
Biochemical methane potential
Kinetic modeling

ABSTRACT

Methane (CH_4) production from anaerobic digestion of solid and liquid agro-industrial wastes is an attractive strategy to meet the growing need for renewable energy sources and promote environmentally appropriate disposal of organic wastes. This work aimed at determining the CH_4 production potential of six agro-industrial wastewaters (AWW), evaluating the most promising for methanization purposes. It also aims to provide kinetic parameters and stoichiometric coefficients of CH_4 production and define which kinetic models are most suitable for simulating the CH_4 production of the evaluated substrates. The AWW studied were swine wastewater (SW), slaughterhouse wastewater (SHW), dairy wastewater (DW), brewery wastewater (BW), fruit processing wastewater (FPW), and residual glycerol (RG) of biodiesel production. RG was the substrate that showed the highest methanization potential. Exponential kinetic models can be efficiently applied for describing CH_4 production of more soluble substrates. On the other hand, logistic models were more suitable to predict the CH_4 production of more complex substrates.

1. Introduction

Nowadays, the recovery of value-added by-products in sanitary and agro-industrial wastewater treatment plants has received much attention. In this perspective, methane (CH_4) production from anaerobic digestion of wastewater is an attractive strategy for obtaining renewable energy, thus reducing dependence on fossil fuels (Andriamanohiarisoamanana et al., 2018; Dollhofer et al., 2018). Anaerobic digestion is potentially beneficial to society, being a sustainable approach to waste management and energy recovery from abundant liquid and solid raw materials (Ahmadi et al., 2020; Scarlat et al., 2018). Besides, controlled biomethanization of agro-industrial effluents can help avoid environmental problems, such as odors generation, the proliferation of rodents and insects, and water bodies eutrophication caused by incorrect final disposal of these organic wastes (Córdoba et al., 2018).

In this context, CH_4 is considered a clean, flammable, and high-calorific fuel that can be applied to generate electricity via heat transfer and steam, as a vehicle fuel, and for injection into the natural gas network for industry and household applications (Khan et al., 2017; Silva et al., 2020). CH_4 content in biogas varies with the substrate's physical-chemical properties (Li et al., 2011). Therefore, when considering waste viability as raw material for a biogas generation plant, it is necessary to understand the kinetics and extension of CH_4 production (Mirmohamadsadeghi et al., 2019). In this context, the biochemical methane potential (BMP) assay is already a widely used and well-described literature method to assess CH_4 production from different substrates (Jingura and Kamusoko, 2017).

The BMP test can provide the kinetic parameters that govern CH_4 production, such as substrate degradation rate (k), production (P) and maximum CH_4 productivity (μ_m), and the presence or absence of a delay phase (lag phase − λ). It can also be applied for stoichiometric production coefficients calculation, which can estimate CH_4 production in anaerobic treatment units (Kafle and Chen, 2016; Pellera and Gidarakos, 2016).

☆ This paper has been recommended for acceptance by Jörg Rinklebe.

* Corresponding author. Department of Hydraulic and Environmental Engineering, Campus do Pici, Bloco 713. Pici., CEP: 60455-900, Fortaleza, Ceará, Brazil.
E-mail address: andre23@ufc.br (A.B. dos Santos).

https://doi.org/10.1016/j.envpol.2021.116876
0269-7491/

Moreover, the BMP test enables the study of the Cumulative Methane Production Curve (CMPC) generated by the substrate biomethanization (Çetinkaya and Yetilmezsoy, 2019). CMPCs have a sigmoidal shape when the substrate has a slow production (lag phase) in the beginning, followed by a fast (exponential phase) and by stabilization (stationary) production. In contrast, exponential CMPCs have a short or nonexistent lag phase (Ware and Power, 2017). The CMPC shape indicates the substrate's biodegradability characteristics, the biomethanization kinetics, the methanogenic microorganisms' performance, and the inhibitory intermediate product generation, such as long-chain carboxylic acids (LCCA) (Sun et al., 2015).

Despite extensive research on the anaerobic digestion of agro-industrial wastes, the optimal performance is rarely achieved due to the lack of BMP data and kinetic analysis, often leading to empiricism in systems design and operation (Yang et al., 2016). Therefore, kinetic modeling of CH_4 production has gained attention to help in the drawbacks mentioned above and the comprehension of mass and energy balances (Çetinkaya and Yetilmezsoy, 2019).

Mathematical modeling is an alternative to improving anaerobic biodegradation process knowledge, providing data for reactor design, operation, and performance prediction (Abu-Reesh, 2014; Turkdogan-Aydinol et al., 2011). Technical literature presents several approaches to predict substrate degradation and anaerobic bioproducts generation (Kythreotou et al., 2014; Rincón et al., 2013). However, there is still no consensus on which model must be used for each substrate, the latter varying in composition (COD, soluble and particulate fractions etc.). Therefore, it is necessary to carry out BMP tests to collect specific data for feeding software applied to bioprocess simulation and control (Jiménez-González and Woodley, 2010).

Thus, this work aimed at determining the CH_4 production potential of six agro-industrial wastewaters (AWW), evaluating the most promising for methanization purposes. It also aims to provide kinetic parameters and stoichiometric coefficients of CH_4 production and define which kinetic models are most suitable for simulating the CH_4 production of the evaluated substrates.

2. Materials and methods

2.1. Substrates and inoculum

As substrates for the BMP tests, six different AWW were used: swine wastewater (SW), slaughterhouse wastewater (SHW), dairy wastewater (DW), brewery wastewater (BW), fruit processing wastewater (FPW), and residual glycerol (RG) of biodiesel production. Besides, two easily degradable carbon sources were used as substrates for comparative purposes: glucose − GL and volatile fatty acids (VFA). The VFA solution consisted of acetic acid (HAc), propionic acid (HPr), and butyric acid (HBu) in the proportion of 1: 1: 1 gCOD. Physical-chemical characterization analyses were performed according to Standard Methods for the Examination of Water and Wastewater (APHA, 2017). (Table S1). The anaerobic biomass used as inoculum (37.9 ± 0.6 gTVS L^{-1}; 18.0 ± 1.0 gTFS L^{-1}) was obtained from a sewage treatment plant situated in Fortaleza city, Ceará, Brazil.

2.2. BMP assays

Three batch reactors (work reactors) were used for each substrate, and three endogenous control reactors (blank assays) were used for inoculum. Such controls were performed to assess residual CH_4 production due to endogenous decay and contained only inoculum, basal medium, and buffer, i.e., medium without a carbon source as a substrate. The BMP was determined by subtracting CH_4 production from the endogenous control reactors (blank tests) by the gross CH_4 output from the working reactors (Filer et al., 2019; Holliger et al., 2016).

Three batch flasks were used for each substrate in the BMP assays. The reactors consisted of borosilicate glass, with 110 mL of total volume (50 mL reaction volume and 60 mL headspace). The substrate/inoculum ratio (S/I) applied was 0.60 ± 0.02 gCOD gVS^{-1} (Çetinkaya and Yetilmezsoy, 2019). The basal medium consisted of macro and micronutrients added in adequate concentrations (Angelidaki et al., 2009). The initial pH was corrected to 7.0 with 1 N NaOH, and, subsequently, sodium bicarbonate ($NaHCO_3$) was added as a buffer in the proportion of 1 g of buffer for each 1 g of COD. Gaseous nitrogen (N_2) was used as the purge gas for 1 min for each flask (Mshandete et al., 2004). The flasks were kept at 35 °C under orbital shaking at 150 rpm (Córdoba et al., 2018; Khalid et al., 2011). The experiment was completed only when it was observed that the daily CH_4 production for three consecutive days was less than 1% of the accumulated CH_4 volume, which occurred on the 35th day (Holliger et al., 2016).

On days 0, 7, 14, 21, 28, and 35 of the experiment, pressures in the reactor headspace were determined by employing a manometric pressure transmitter (Warme LTDA, Brazil) to quantify the CH_4 volume generated. At the beginning (zero-day) and the end of the batch (35th day), chemical oxygen demand analyzes for organic matter were performed. Solids series was also determined, as well as VFA. On the 35th day, a 1 mL sample of biogas was analyzed by gas chromatography to determine CH_4, H_2, CO_2, and H_2S average concentrations. Biogas samples were collected using gas-tight syringes (SampleLock syringe, Hamilton Company, USA). Biogas composition and VFA concentrations were determined by gas and liquid chromatography, respectively, using methods previously described by Morais et al. (2020a).

Specific Methanogenic Activity (SMA, $gCOD_{CH4}$ gVS^{-1} d^{-1}) parameter was calculated according to Angelidaki et al. (2009) using mathematical models, such as Modified Gompertz, Logistics, and Transference, to estimate the maximum CH_4 production rate (μ_m, $mLCH_4$ d^{-1})..

2.3. Experimental design and data processing and kinetic study

The experiment was conducted by using a completely randomized design (CRD), carried out in a balanced way with eight treatments (SW, SHW, DW, BW, FPW, RG, GL, and VFA) in three replications, resulting in 24 experimental plots that were randomly allocated in the incubator to promote spatial randomness. The response variables referring to the BMP assays were: 1) yield of CH_4 production by removed COD ($Y1_{CH4}$, $mLCH_4$ $gCOD_R^{-1}$), 2) yield of CH_4 production by applied COD ($Y2_{CH4}$, $mLCH_4$ $gCOD_A^{-1}$), 3) biogas composition, 4) percentage of the initial organic matter converted to methane (COD_{CH4}), cell growth (COD_{VSS}) and VFA (COD_{VFA}), and 5) non-biodegraded organic matter at the end of the test (COD_{NB}).

Data for each repetition were assessed with descriptive statistics to check outliers between repetitions of the same treatment. As anomalies were not observed and low standard deviation and coefficient of variation were found, all collected data were used, presenting the mean and standard deviation to represent the CH_4 production profile in each treatment. The response variables were applied to the analysis of variance (one-way ANOVA) with a 99% confidence level and 1% probability ($p < 0.01$) and then to the comparison test between Scott-Knott means, performed using the SISVAR statistical software (Ferreira, 2019). Within the same response variable analyzed, the average values followed by the same letters belong to the same statistical group, according to the

Table 1
Kinetic models selected to describe methane production.

Kinetic model	Kinetic model equation
First-order exponential	$P_t = P[1 - exp(-kt)]$
Fitzhugh	$P_t = P[1 - exp(-kt)^n]$
Cone	$P_t = \frac{P}{1 + (kt)^{-n}}$
BPK	$P_t = P\left\{1 - exp\left[(m-1)\left(\frac{t}{t_0}\right)^{1/m}\right]\right\}$ $\mu_m = \frac{P\,exp(m)(1-m)}{e.m.t_0}$ $\quad k = \frac{exp(m)(1-m)}{e.m.t_0}$
Monomolecular	$P_t = P[1 - \exp(-k(t-\lambda))]$
Modified Gompertz	$P_t = Pexp\left\{-exp\left[\frac{\mu_m e}{P}(\lambda - t) + 1\right]\right\}$
Logistic	$P_t = \frac{P}{1 + exp\left[\frac{4\,\mu_m(\lambda - t)}{P} + 2\right]}$
Transference	$P_t = P\left\{1 - exp\left[-\frac{\mu_m(t-\lambda)}{P}\right]\right\}$
Richards	$P_t = P\left\{1 + v.exp(1+v).exp\left[\frac{\mu_m}{P}.(1+v)\left(1+\frac{1}{v}\right)(\lambda - t)\right]\right\}^{(-1/v)}$

Legend: P_t: methane accumulated during the incubation period (mL). P: volume of methane generated during the experiment (mL). k: methane production rate constant (d^{-1}). t: digestion time (d). n: shape constant (dimensionless). m: shape constant of the BPK model (dimensionless). e: euler number (dimensionless). t_0: time when the methane production rate is maximum (d). λ: time of the lag phase (d). μ_m: maximum rate of methane production (mL d^{-1}). v: Richards model constant (dimensionless).

Scott-Knott test at the 5% probability level. Principal Component Analysis (PCA) was used to identify the most important components that affect biogas quality and CH_4 production potential. This analysis was performed using the PAST 3 software (Hammer et al., 2001).

The kinetics models selected to describe CH_4 production were: First-order exponential, Monomolecular, Fitzhugh, Cone, BPK, Logistic, Transference, Richards, and Modified Gompertz (Table 1) (Morais et al., 2020a). These simple models are based on the kinetics of the limiting stage of the anaerobic digestion process, which is a complex bioprocess that involves different microbial groups with different kinetic activities. However, the application of these models is already consolidated in the technical literature, showing efficacy to simulate methane production in anaerobic microbiomes (Rincón et al., 2013; Yang et al., 2016).

The most efficient model for describing CH_4 production, the values of kinetic parameters and the coefficient of determination values (R^2), the normalized root-mean-square error (NRMSE), and the Akaike Information Criterion (AIC), were determined according to Lima et al. (2018). Data obtained from kinetic modeling were applied to plot curves using Origin 8.1 software (OriginLab Corporation, Northampton, MA, USA). BMP experimental assay's scheme can be seen in Fig. 1.

3. Results and discussion

3.1. Methane production potential and yields

In the variance analysis, values obtained for the coefficient of experimental variation (CV) at a level of 1% probability indicate experimental precision (Table 2). No statistically significant difference between treatments concerning the variable S/I ratio was found, allowing for the null hypothesis H_0 (Table 2). Therefore, it is possible to state that all reactors, regardless of substrate and culture conditions (basal medium and buffer), were subjected to the same initial S/I, indicating homogeneity between treatments. Therefore, any statistically significant difference is due to the composition of the substrates tested. Regarding the response variables $Y1_{CH4}$, $Y2_{CH4}$, CH_4, and CO_2, data in Table 2, according to the F test at 1% probability level, evidence significant differences between treatments, therefore rejecting the null hypothesis H_0. Thus, it must be at least a significant contrast between the means of treatments concerning these response variables.

Scott-Knott test was then used to identify treatments statistically different by comparing the eight treatments' averages (Table 3). The average values of CH_4 production by removed COD ($Y1_{CH4}$) from each substrate were numerically higher than those of the CH_4 output by applied COD ($Y2_{CH4}$), also highlighting the different forms of grouping (Table 3). Therefore, factors that influence the stoichiometric coefficient $Y1_{CH4}$ are different from those that influence the $Y2_{CH4}$.

In terms of CH_4 production by removed COD ($Y1_{CH4}$) and CH_4 concentration, the Scott-Knott test separated the substrates into two distinct groups. Substrates with the highest $Y1_{CH4}$ values also presented biogas with the highest CH_4 content. SW, DW, and RG showed $Y1_{CH4}$ and CH_4 highest values, which were statistically equal to each other and statistically equivalent to CH_4 production from VFA. The SHW, BW, and FPW substrates had the lowest $Y1_{CH4}$ and CH_4 values (except BW for CH_4 concentrations), which were statistically equal to each other and statistically equivalent to CH_4 production with GL.

The high $Y1_{CH4}$ obtained in SW assay can be justified by a significant number of microorganisms in this wastewater, which can contribute to the syntrophic activity between hydrolytic, acidogenic and methanogenic microorganisms and, consequently, favor the biomethanization process (Cheng et al., 2018; Ding et al., 2017). On the other hand, SHW presented the lowest potential for CH_4 production since lower values of $Y1_{CH4}$ and $Y2_{CH4}$ were obtained. Such behavior probably occurred due to substrate composition, formed by blood generated in the slaughter of cattle. It may also contain heavy metals and residues of cleaning agents and veterinary medical products, negatively affecting methanization efficiency (Pereira et al., 2016). Besides, SHW is generally characterized by having both a high LCCA content, which can temporarily inhibit methanogenesis and high concentrations of proteins that can limit the hydrolysis rate by having slow biodegradation (Kafle and Kim, 2012; Maya-Altamira et al., 2008).

In terms of CH_4 production by applied COD ($Y2_{CH4}$), the Scott-Knott test separated the substrates into four groups, with RG and SHW having the highest and lowest $Y2_{CH4}$ values observed,

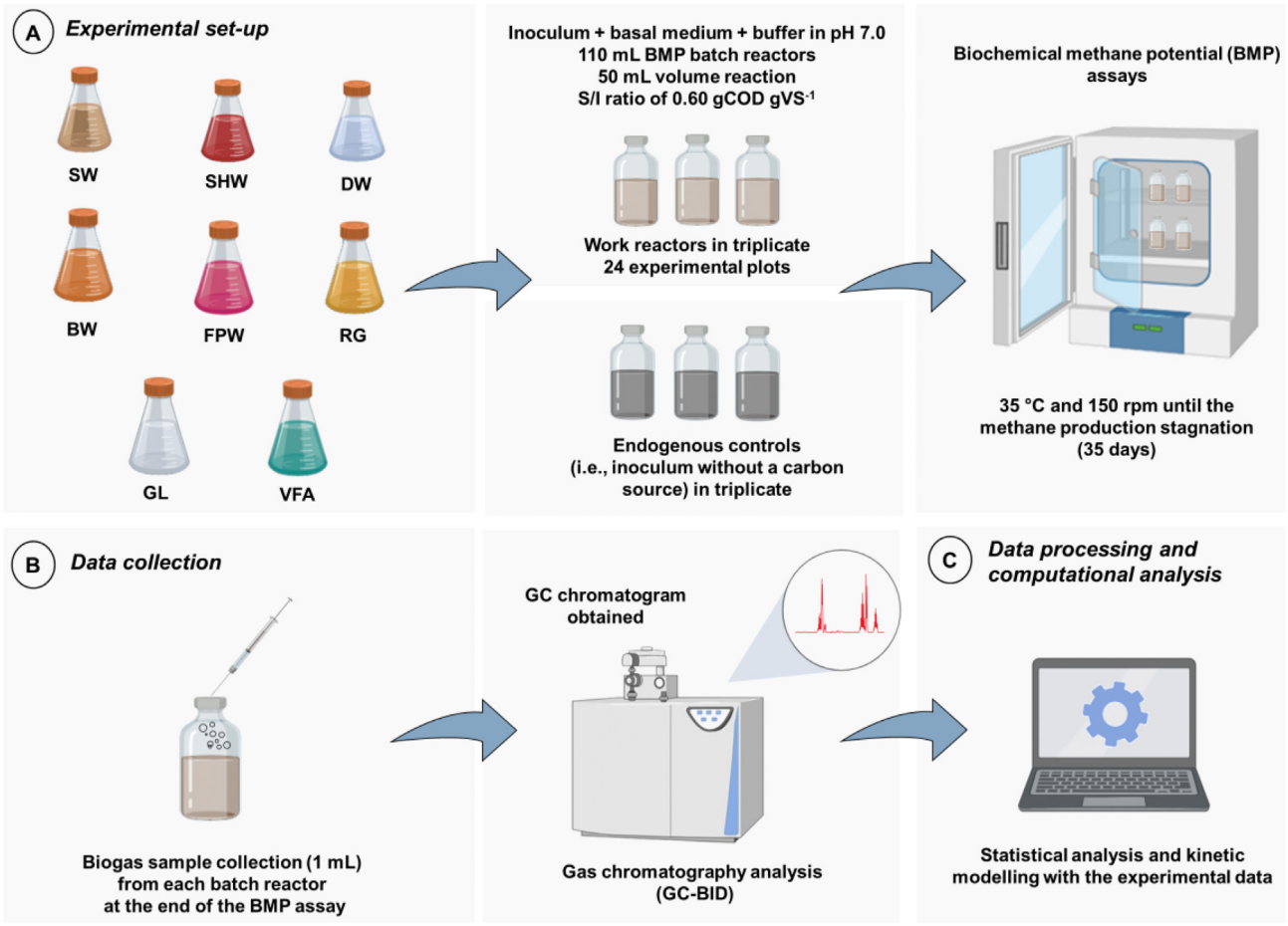

Fig. 1. Biochemical methane potential (BMP) experimental assay's scheme. Legend: SW: swine wastewater. SHW: slaughterhouse wastewater. DW: dairy wastewater. BW: brewery wastewater. FPW: fruit processing wastewater. RG: residual glycerol. GL: glucose. VFA: volatile fatty acids. (A) Experimental set-up; (B) Data collection; (C) Data processing and computational analysis.

Table 2
One-way ANOVA summary.

Variation source	DF	S/I	$Y1_{CH4}$	$Y2_{CH4}$	CH_4	CO_2
Substrate	**7**	**0.0002^{ns}**	**5345.82****	**5984.29****	**12.41****	**11.10****
Error	**16**	**0.0004**	**514.66**	**145.69**	**1.43**	**0.08**
CV (%)		**3.42**	**7.1**	**5.44**	**16.92**	**9.29**

Legend: DF: Degrees of freedom. CV: Coefficient of variation. S/I: Substrate/inoculum ratio ($gCOD_A\ gVS^{-1}$). $Y1_{CH4}$: Yield of CH_4 production by removed COD ($mLCH_4\ gCOD_R^{-1}$). $Y2_{CH4}$: Yield of CH_4 production by applied COD ($mLCH_4\ gCOD_A^{-1}$). CH_4: CH_4 concentration in the biogas (mmol L^{-1}). CO_2: Concentration of carbon dioxide in the biogas (mmol L^{-1}). ns: There is no statistical difference between treatments. ** Significant at the 1% probability level by the F test ($p < 0.01$).

Table 3
Mean values of the response variables of the BMP assay.

Substrates	S/I	$Y1_{CH4}$	$Y2_{CH4}$	CH_4	CO_2
SW	0.60^a	352.0^a	248.4^a	8.27^a	1.78^a
SHW	0.60^a	259.2^b	129.8^b	5.71^b	2.15^a
DW	0.58^a	349.0^a	222.1^c	8.86^a	4.00^b
BW	0.60^a	278.3^b	208.6^c	9.17^a	5.80^c
FPW	0.60^a	283.2^b	227.3^c	4.10^b	0.88^d
RG	0.60^a	358.7^a	285.4^d	8.39^a	4.56^e
GL	0.58^a	299.8^b	242.0^a	4.40^b	4.54^e
VFA	0.58^a	366.9^a	210.6^c	7.68^a	0.65^d

Legend: Within the same response variable analyzed, the means followed by the same letters belong to the same group, according to the Scott-Knott test at the 5% probability level. S/I: Substrate/inoculum ratio ($gCOD_A\ gVS^{-1}$). $Y1_{CH4}$: Yield of CH_4 production by removed COD ($mLCH_4\ gCOD_R^{-1}$). $Y2_{CH4}$: Yield of CH_4 production by applied COD ($mLCH_4\ gCOD_A^{-1}$). CH_4: CH_4 concentration in the biogas (mmol L^{-1}). CO_2: Concentration of carbon dioxide in the biogas (mmol L^{-1}).

respectively. DW, BW, and FPW showed CH_4 production equivalent to the VFA mixture and SW equivalent to GL. It is interesting to note that the variable $Y2_{CH4}$ has no grouping relationship with the variable CH_4 (Table 3).

Due to the statistical similarity of SW with GL and DW, BW, and FPW with VFA, $Y2_{CH4}$ can be influenced by the substrates' physical-chemical characteristics. This possible correlation was explored by using PCA analysis (Fig. 2). The physical and chemical factors that most explained the principal components were the raw concentration of oils and greases (OG), the percentages between the soluble (CODS) and particulate (CODP) fractions of organic matter that characterize the total applied COD (CODT), and the proportions between total dissolved (TDS) and suspended (VSS) solids, relative to the amount of total solids (TS) present in the substrates.

The perceptual map presented in Fig. 2 helps assess the relationship between variables since components 1 and 2 explain 81.8% of the data variability. Technical literature reports that principal components must describe at least 70% of the system variance (Pereira et al., 2019). Therefore, the perceptual map allows us to identify how the substrates are ordered and their relationship among the variables OG, COD_S/COD_T, COD_P/COD_T, TDS/TS, and VSS/TS.

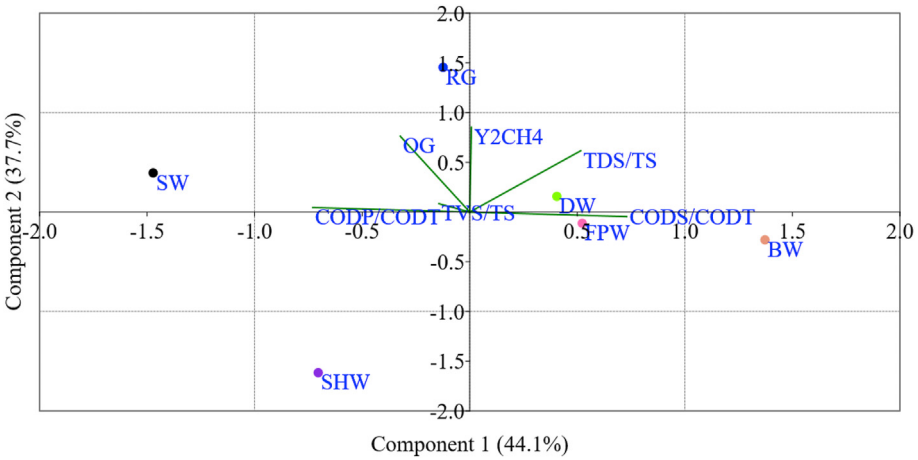

Fig. 2. Perceptual map with the Principal Component Analysis (PCA). Legend: Principal Component 1 (PC1, x-axis): segregated the substrates into more soluble and more particulate. Principal Component 2 (PC2, y-axis): segregated the substrates by the highest and lowest concentrations of OG and $Y2_{CH4}$.

The $CODs/COD_T$ and COD_P/COD_T ratios were the variables that presented the highest importance in the principal component 1 (PC1, x-axis), segregating the substrates into more soluble (DW, BW, FPW, and RG) and more particulate (SW and SHW). Principal component 2 (PC2, y-axis) segregated the substrates by the highest (RG, SW, and DW) and lowest (SHW, FPW, and BW) OG and $Y2_{CH4}$ concentrations, indicating that substrates with the highest OG concentrations were those that obtained higher $Y2_{CH4}$. Despite the slow anaerobic degradation of fats, its energy potential is higher than the energy provided by proteins and carbohydrates degradation, which may have favored CH_4 production (Ware and Power, 2017).

Therefore, it is possible to state that substrates with more than 60% of COD_T as COD_S fraction showed CH_4 production by applied COD similar to that of the VFA substrate. Substrates with more than 80% of COD_T as COD_P fraction and high OG concentrations, such as SW, showed CH_4 production by COD applied similar to that of GL substrate (Table 3).

PCA's perceptual map also indicates that OG elements and COD_P/COD_T ratio are positively correlated with each other, which means that substrates with high OG and COD_P/COD_T concentrations were the ones with the highest $Y2_{CH4}$. RG and SHW substrates are in opposite positions in PC2, being negatively correlated by the variable OG, suggesting that different physical and chemical characteristics govern the $Y2_{CH4}$ of these substrates. Moreover, it shows that RG and SHW obtained the highest and lowest $Y2_{CH4}$ values observed, respectively.

It is accepted that $Y2_{CH4}$ is governed by COD fractions directed towards CH_4 production (COD_{CH4}), VFA (COD_{VFA}), and cell growth (COD_{VSS}) during the anaerobic process. Therefore, in terms of mass and energy conservation, the data presented in Table 4 helps to understand the flow of each organic matter fraction that was applied (COD_A) and the $Y2_{CH4}$ values obtained.

The most soluble substrates (DW, BW, and FPW) are grouped concerning the organic matter fraction used for CH_4 production (Table 4), showing their statistical correlation with $Y2_{CH4}$ (Table 3). The anaerobic process with BW and FPW presented more than 20% of the organic matter used for cell growth, and 30% of the COD applied in the DW tests remained as VFA at the end of the experiment. Coelho et al. (2020) observed that DW has a high potential for acidification under acidogenic conditions (with methanogenesis inhibition). The authors have achieved a yield of 0.66 g $gCOD_A^{-1}$ acids (corresponding to 0.83 gCOD $gCOD_A^{-1}$) in batch tests with mixed culture. Thus, it is clear that in the anaerobic digestion of the most soluble substrates (DW, BW, and FPW), organic matter consumption for cell growth and VFA formation had a greater influence on the anaerobic process compared to the methanization of more complex substrates (e.g., SW), which reducing the organic matter available for the biomethanization process, decreasing the $Y2_{CH4}$ values (Table 3).

Table 4
Average values of the organic matter targeting variables.

Substrates	COD_{VFA}	COD_{CH4}	COD_{VSS}	COD_{NB}
SW	27.3^a	62.7^a	8.0^a	2.0^a
SHW	33.3^c	33.0^c	17.3^b	16.7^b
DW	30.0^a	56.0^b	7.7^a	5.7^a
BW	17.0^b	53.0^b	22.7^b	7.3^a
FPW	16.3^b	57.7^b	23.0^b	3.3^a
RG	17.0^b	72.0^d	7.3^a	3.0^a
GL	15.0^b	61.3^a	19.7^b	4.0^a
VFA	41.0^d	53.0^b	4.3^c	1.3^c

Legend: Within the same response variable analyzed, the means followed by the same letters belong to the same group, according to the Scott-Knott test at the 5% probability level. Data in percentage (%). Percentage of the initial organic matter converted to methane (COD_{CH4}), cell growth (COD_{VSS}), and volatile fatty acids (COD_{VFA}). COD_{NB}: non-biodegraded organic matter at the end of the test.

The anaerobic test with SHW showed the lowest potential for CH_4 production if compared with the other substrates (33%). At the end of the experiment, on average, 33.3% of the applied COD remained as VFA, indicating that SHW has a good potential for VFA production, as previously reported by Plácido and Zhang (2018) and Morais et al. (2020b). These authors evaluated agitated batch reactors using SHW as a substrate for carboxylic acid production potential test and found a high conversion of the organic matter applied for VFA formation. Therefore, SHW resulted in a lower COD directed towards CH_4 formation and subsequent low $Y2_{CH4}$ value (Table 3). On the other hand, RG and SW substrates had the highest fractions of organic matter intended for CH_4 production, with conversion efficiencies of 72.0 and 62.7%, respectively. They also presented low values for cell growth and VFA formation (Table 4), resulting in the highest $Y2_{CH4}$ values (Table 3).

BW provided the highest CO2 concentration in terms of biogas composition, followed by RG, whose CO_2 concentration was equal to that found with GL. The lowest CO_2 concentration in the biogas was found for FPW, which was equal to that achieved with the VFA mixture (Table 3). H_2S concentrations in the biogas were (mmol L^{-1}): 0.0064 (SW), 0.0146 (SHW), 0.0111 (DW), 0.0064 (BW), 0.0013 (FPW), and 0.0054 (RG). Gas samples of VFA and GL batch assays did

not reveal H_2S, and hydrogen (H_2) was never detected, regardless of the substrate.

Based on the BMP assays, RG was the substrate with the highest potential for CH_4 production by removed COD and applied COD. Also, the use of these wastewaters may require biogas purification strategies in methanization plants that aim high content of CH_4 in the biogas (for instance, above 90–95%) (Khan et al., 2017).

3.2. Kinetic study of methane production

3.2.1. Glucose, VFA, and SMA study

Glucose's CMPC was exponentially shaped (Fig. 3A). GL showed a generation of 32.80 ± 2.5 $mLCH_4$ and a technical digestion time (T80) of 10 days. Generally, T80 is a parameter applied to evaluate biomethanization efficiency and estimate the hydraulic retention

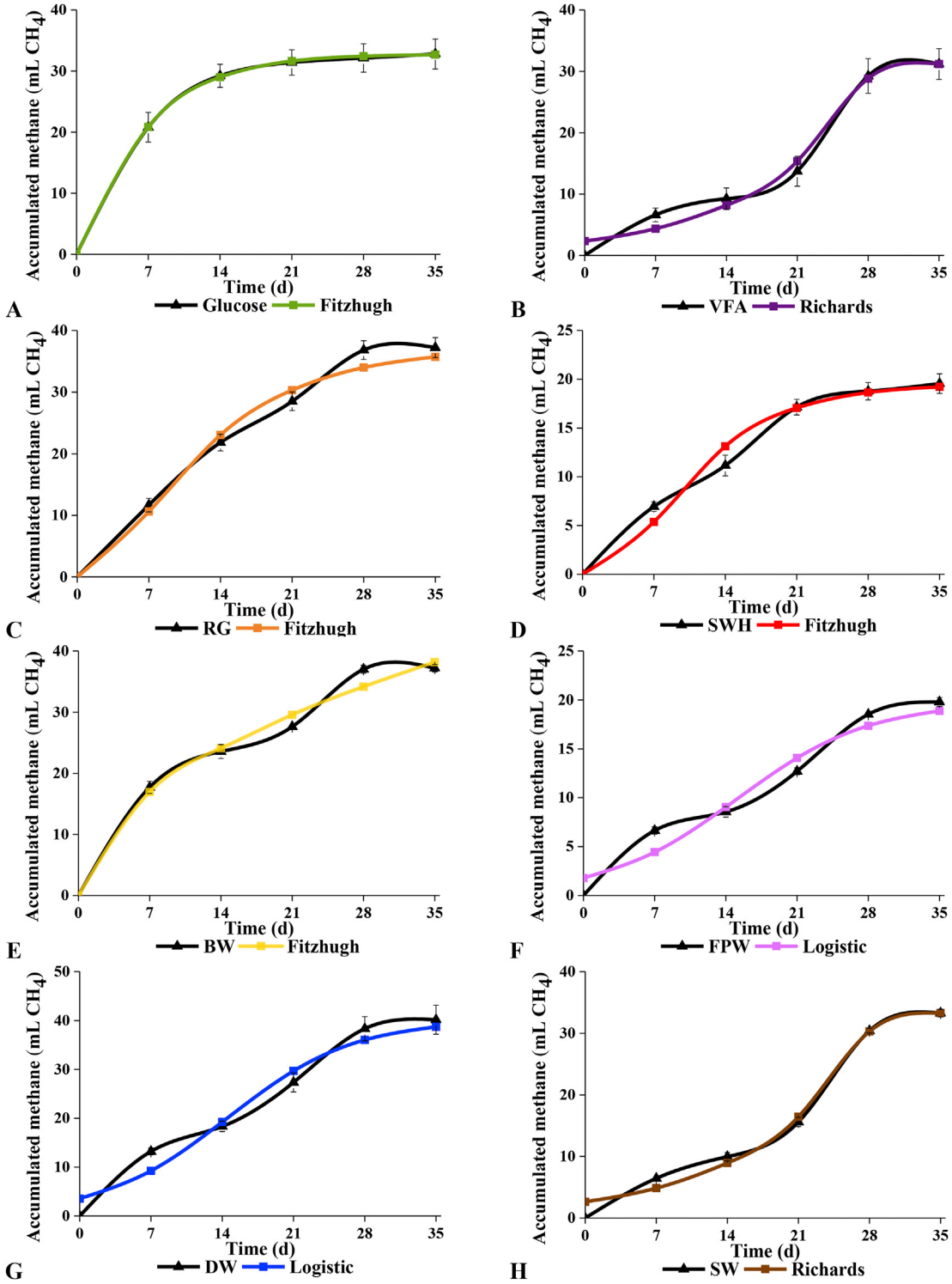

Fig. 3. Cumulative Methane Production Curve (CMPC) and curves generated by the best fit kinetic models. Legend: (A) Glucose (Fitzhugh model). (B). VFA (Richards model). (C) RG (Fitzhugh model). (D) SHW (Fitzhugh model). (E) BW (Fitzhugh model). (F) FPW (Logistic model). (G) DW (Logistic model). (H) SW (Richards model).

Table 5
Mean values of parameters estimated by kinetic modeling.

Model	Parameters	SW	SHW	DW	BW	FPW	RG	GL	VFA
First-order exponential	**k (d^{-1})**	0.046	0.079	0.062	0.069	0.059	0.072	0.149	0.046
	R^2	0.831	0.964	0.935	0.948	0.925	0.960	0.999	0.812
	NRMSE	15.057	6.828	8.962	7.800	9.491	7.175	0.884	16.005
	AIC	21.337	5.468	17.370	14.787	9.569	13.794	−12.859	21.297
Monomolecular	**k (d^{-1})**	0.050	0.083	0.064	0.082	0.061	0.075	0.149	0.050
	λ (d)	1.612	0.627	0.543	0.000	0.507	0.546	0.014	1.536
	R^2	0.843	0.966	0.937	0.968	0.927	0.963	0.999	0.822
	NRMSE	14.523	6.694	8.818	6.123	9.382	6.933	0.879	15.554
	AIC	22.904	7.231	19.176	13.880	11.431	15.382	−10.917	22.955
Fitzhugh	**k (d^{-1})**	0.114	0.147	0.091	0.002	0.085	0.112	0.168	0.114
	n	5.089	2.922	1.835	0.512	1.746	2.060	1.231	5.232
	R^2	0.923	0.979	0.956	0.986	0.943	0.985	0.999	0.899
	NRMSE	10.188	5.295	7.398	4.065	8.252	4.406	0.548	11.735
	AIC	18.649	4.417	17.070	10.964	9.891	9.942	−16.583	19.573
Cone	**k (d^{-1})**	0.054	0.099	0.081	0.000	0.078	0.092	0.180	0.053
	n	3.672	2.269	2.115	0.539	2.048	2.291	2.337	3.829
	R^2	0.917	0.973	0.935	0.986	0.921	0.974	0.999	0.895
	NRMSE	10.516	5.919	8.933	4.083	9.759	5.847	0.600	11.983
	AIC	19.030	5.754	19.332	11.018	11.904	13.337	−15.508	19.825
BPK	**m**	0.942	0.870	0.895	0.844	0.888	0.862	0.739	0.899
	t_0 (d)	1.349	1.889	1.884	2.248	2.127	2.209	2.373	2.448
	μ_m (mL d^{-1})	1.440	1.361	2.243	2.621	1.047	2.343	3.754	1.295
	k (d^{-1})	0.043	0.070	0.056	0.070	0.053	0.063	0.114	0.042
	R^2	0.831	0.964	0.935	0.968	0.925	0.960	0.999	0.812
	NRMSE	15.057	6.828	8.962	6.123	9.491	7.175	0.884	16.005
	AIC	23.337	7.468	19.370	13.880	11.569	15.794	−10.859	23.297
Logistic	**μ_m (mL d^{-1})**	1.495	1.150	1.611	1.683	0.756	1.742	4.404	1.411
	λ (d)	8.124	2.950	2.053	0.000	2.033	1.817	2.339	8.321
	R^2	0.960	0.975	0.965	0.926	0.956	0.979	0.983	0.942
	NRMSE	7.361	5.746	6.600	9.319	7.243	5.268	4.587	8.920
	AIC	14.750	5.397	15.700	18.921	8.326	12.086	8.904	16.283
Transference	**μ_m (mL d^{-1})**	1.656	1.616	2.570	3.064	1.205	2.784	4.879	1.548
	λ (d)	1.612	0.627	0.543	0.000	0.507	0.546	0.014	1.536
	R^2	0.843	0.966	0.937	0.968	0.927	0.963	0.999	0.822
	NRMSE	14.523	6.694	8.818	6.123	9.382	6.933	0.879	15.554
	AIC	22.904	7.231	19.176	13.880	11.431	15.382	−10.917	22.955
Richards	***v***	87.470	1.253	1.199	65.073	2.763	0.754	0.005	122.479
	μ_m (mL d^{-1})	2.837	1.084	1.702	2.220	0.960	1.581	0.042	2.762
	λ (d)	16.896	2.127	2.274	6.906	4.087	1.660	0.833	17.236
	R^2	0.987	0.979	0.965	0.882	0.958	0.981	0.994	0.982
	NRMSE	4.120	5.273	6.595	11.776	7.103	5.003	2.786	4.958
	AIC	9.784	6.367	17.691	23.730	10.092	13.466	4.918	11.234
Modified Gompertz	**μ_m (mL d^{-1})**	1.422	1.018	1.645	1.853	0.767	1.824	3.373	1.319
	λ (d)	6.401	1.303	1.122	0.000	0.965	1.370	0.866	6.328
	R^2	0.932	0.986	0.962	0.947	0.951	0.986	0.994	0.910
	NRMSE	9.511	4.302	6.848	7.881	7.648	4.296	2.765	11.069
	AIC	17.825	1.924	16.142	16.910	8.979	9.638	2.827	18.872

Legend: k: velocity constant (d^{-1}). t: digestion time (d). n: shape constant (dimensionless). m: shape constant of the BPK model (dimensionless). e: Euler number (dimensionless). t_0: time when the methane production rate is maximum (d). λ: lag phase time (d). μ_m: maximum rate of methane production (mL d^{-1}). v: Richards model constant (dimensionless). R^2: determination coefficient. NRMSE: normalized root-mean-square error. AIC: Akaike Information Criterion.

time (HRT) in wastewater treatment using continuous flow reactors (Córdoba et al., 2018; Sanjaya et al., 2016).

The Fitzhugh model showed the best fit for CH_4 production data from GL (Table 5). The Cone and Fitzhugh models indicated the presence of a lag phase (Cone constant n > 1) (Lima et al., 2018). However, the Modified Gompertz and Monomolecular models estimate low values for delay phase (λ): 0.866, and 0.014 d, respectively. The estimation indicates that the biodegradable fraction was readily consumed by the microorganisms, confirming GL's expected high biodegradability (Kainthola et al., 2019). Besides, very low or negative values of the delay phase indicate that CH_4 production may have occurred immediately after inoculation, considerably reducing the time required to reach the exponential phase (Jijai et al., 2016). The maximum rate of CH_4 production (μ_m) was estimated by the Transference model (4.8 $mLCH_4$ d^{-1}).

VFA solution's CMPC (Fig. 3B) was best described by the Richards model (Table 5). The BMP assays generated 31.2 ± 2.5 $mLCH_4$ for VFA. For this substrate, T80 was superior to that found for GL, requiring approximately 25 days to reach the production of 80% of the total CH_4 volume. The μ_m was estimated by the Richards model (2.76 $mLCH_4$ d^{-1}).

The high T80 obtained and low μ_m estimated by the kinetic models can be validated by the low SMA values obtained for the inoculum used. SMA values of 12.35 ± 1.1 $mLCH_4$ gVS^{-1} d^{-1} (0.031 ± 0.003 $gCOD_{CH4}$ gVS^{-1} d^{-1}) and 21.7 ± 2.1 $mLCH_4$ gVS^{-1} d^{-1} (0.055 ± 0.005 $gCOD_{CH4}$ gVS^{-1} d^{-1}) were obtained when VFA solution and GL were used, respectively. Therefore, the inoculum has low methanogenic activity and low syntrophic capacity in the conversion of HPr and HBu into HAc, evidenced by the low SMA value obtained with the VFA solution and also by the high percentages of organic matter remaining in VFA form at the end of the tests with SW (27.3%), SHW (33.3%), DW (30.0%), and even when the VFA solution was the substrate (41.0%) (Table 4).

According to Aquino et al. (2007), microorganisms syntrophic activity evaluation is essential for anaerobic reactors operation. The low syntrophic interactions in converting propionate and butyrate

to acetate can decrease the anaerobic reactor efficiency due to methanogenic microorganisms preferentially producing CH_4 from acetate.

Lozada et al. (2008) determined the SMA of granular anaerobic sludge from a UASB reactor treating paper and cellulose wastewaters. The authors reported an SMA value of 0.2 $gCOD_{CH4}\ gVS^{-1}\ d^{-1}$ when they used VFA as a substrate in a batch test with a S/I of 1.0 $gCOD\ gVS^{-1}$. Schneiders et al. (2013), using the same SMA methodology adopted in the current work, found an SMA value of 0.17 $gCOD_{CH4}\ gVS^{-1}\ d^{-1}$, when the VFA was the substrate and a granular anaerobic sludge from a UASB reactor treating wastewater from the food industry was used as inoculum.

Therefore, based on the results published by Lozada et al. (2008) and Schneiders et al. (2013), it is possible to affirm that the inoculum used in the BMP tests of this work has SMA inferior to that of the granular anaerobic sludge, underestimating the CH_4 production potential of the evaluated substrates. Thus, sludge sources with a higher SMA would provide higher CH_4 production for the tested AWW. However, it is worth mentioning that the operating conditions used, such as the S/I ratio, temperature, type of reactor, and flow regimes, may have influenced the highest SMA values previously reported. Besides, batch reactors with orbital agitation have limitations of mass transfer between the substrate and the microbial aggregates, decreasing SMA (Zinatizadeh et al., 2017).

These limitations may be even more significant than the mass transfer processes in high-rate anaerobic reactors. The specialized biomass formed makes the treatment possible, making the conversion faster (Lier et al., 2016). Furthermore, continuous flow anaerobic reactors with or without immobilized biomass, with or without effluent recirculation, and anaerobic batch reactors with mechanized agitation, allow greater contact of the substrate with the microorganisms, favoring the mechanisms of mass transport and, consequently, substrate methanization (Afridi et al., 2018).

3.2.2. Agro-industrial wastewaters

RG and SHW CMPC's resembled an exponential curve due to the high yield of CH_4 production in the first days, followed by a constant decrease until stabilization (Fig. 3C and D). However, this bioproduct generation occurred slowly for these substrates compared to GL, requiring 21 and 18 days for 80% of the CH_4 volume to be produced from RG and SHW, respectively. RG and SHW biomethanization provided 37.2 ± 1.6 $mLCH_4$ and 19.5 ± 1.0 $mLCH_4$, respectively. The μ_m parameter for these substrates was estimated by the Modified Gompertz Model (1.82 $mLCH_4\ d^{-1}$ for RG and 1.02 $mLCH_4\ d^{-1}$ for SHW). The Fitzhugh model satisfactorily described the CH_4 production of these substrates (Table 5).

The CMPC of BW, FPW, and DW (Fig. 3E, F, and 3G) were characterized by an exponential increase in the first days of the experiment, followed by a sigmoidal form CH_4 production. Generally, in the initial stage of anaerobic digestion, the most easily degradable materials (i.e., carbohydrates) are consumed quickly, causing the CMPC to follow a first-order exponential growth pattern (Rincón et al., 2013). Hydrolysis of more complex organic matter causes a delay in CH_4 production, often expressed by a sigmoid curve (Donoso-Bravo et al., 2010; Li et al., 2012).

Therefore, both exponential and sigmoidal models have successfully described the biomethanization of these substrates, emphasizing the Fitzhugh and Logistics models (Fig. 3E, F, and 3G). The BMP assays generated were ($mLCH_4$) 19.80 ± 0.5, 37.2 ± 0.6, and 40.2 ± 3.0 for FPW, BW, and DW, respectively. The Logistic model estimated the maximum CH_4 production rate for DW (1.61 $mLCH_4\ d^{-1}$) and FPW (0.756 $mLCH_4\ d^{-1}$), while the Transference model calculated 3.06 $mLCH_4\ d^{-1}$ as μ_m for BW. The T80 for these substrates varied from 23 to 25 days, longer than the values observed for GL, RG, and SHW.

Therefore, kinetic models describing exponential functions can be efficiently applied to simulate CH_4 production from more soluble substrates (GL and RG) because they do not consider the presence of a lag phase. Although SHW is characterized as a substrate with a high concentration of particulate organic matter (COD_P/COD_T = 0.54), its faster biomethanization than other substrates provided a CMPC that exponential kinetic models can efficiently describe. However, both exponential and sigmoidal models can explain the biomethanization process of substrates (FPW, BW, and DW) that presented CH_4 production in two stages.

SW's CMPC (Fig. 3H) resembled the sigmoidal form (logistic growth). These curves are characteristic of substrates that have high concentrations of complex organic compounds, such as fats, lignocellulose, or high fractions of organic matter in particulate form and, generally, indicate a slower and gradual CH_4 production, and, consequently, a longer lag phase (Labatut et al., 2011). Therefore, mathematical models that present the phase lag parameter (λ) in their formulations were much suitable to describe the kinetics of CH_4 formation from more complex substrates.

Fat-rich substrates, such as SW, generally have a slower degradation pattern and are more likely to promote biochemical inhibition due to LCCA accumulation from the hydrolysis process. In this case, hydrolysis becomes the limiting phase of anaerobic digestion, influencing the CH_4 formation rate (Labatut et al., 2011). According to Lim et al. (2012), SW is a liquid organic waste with a high content of particulate organic material due to proteins and lipids from animal excrement and undigested food residues. High COD concentrations (18,707 $mgO_2\ L^{-1}$), total nitrogen (361 mg-N L^{-1}), total phosphorus (150 mg-P L^{-1}), and oils and greases (147 mg L^{-1}) obtained in the raw SW characterization used in our tests shows the complexity of this substrate and the high presence of fats (Table S1).

The Richards model was the one that best managed to adapt to CMPC with a sigmoidal shape of SW (Table 5). Unlike the Logistic and Modified Gompertz models, the Richards model has a dimensionless factor (v). This model allows the knowledge about the curve's inflection point to occur at any point between the minimum and maximum asymptote of CH_4 production, allowing a better experimental curve adjustment (Ware and Power, 2017). The lag phase in CH_4 production was estimated at approximately 17 d for SW. This extended period likely indicates a low methanogenic activity caused by a slower degradation of organic matter and the occurrence of some temporary inhibitory process, such as LCCA accumulation (Maamri and Amrani, 2015). The BMP assay with SW generated 33.3 ± 0.6 $mLCH_4$, and the μ_m parameter was estimated by the Richards model (2.84 $mLCH_4\ d^{-1}$). For this substrate, T80 was superior to that found for the most soluble substrates, requiring approximately 27 days to produce 80% of the CH_4 volume.

Based on the results presented and discussed, it can be assumed that most of the particulate wastewaters are biodegraded more slowly and usually have CMPC in sigmoidal form. In contrast, the more soluble wastewaters are biodegraded quickly, presenting CMPC in exponential format. These results can be justified based on mass transport mechanisms in anaerobic reactors, directly influencing the methanization kinetics.

According to Pavlostathis and Giraldo-Gomez (1991), the most soluble substrates are readily available to be transported, through Brownian diffusion, from the wastewater to the microbial aggregates, being catabolized and converted to CH_4. However, during the anaerobic digestion of more particulate substrates, the mass transfer mechanisms are limited due to the need for particle adsorption/aggregation to the biofilm (anaerobic aggregates) and its subsequent hydrolysis. In this case, gravity sedimentation and interception are the main mechanisms of mass transport that

promote particles' collision with the microbial aggregates (Yao et al., 1971).

However, particles' attachment to the biofilm occurs by chemical adhesion mechanisms but is not always successful due to electrostatic repulsion (O'Melia, 1980). Additionally, the particles adsorbed to the biofilm make it challenging to capture soluble substrates due to the decrease in the accessible surface area, reducing the overall conversion.

3.2.3. Methane production rate constant (k)

The k-value reported in the kinetic models' equations can be understood as the speed at which a product – in this case, CH_4 – is generated. This parameter is influenced by the substrate anaerobic biodegradability, the test temperature, and the presence of inhibitory substances. In general, when there are no inhibitory substances, the organic matter present in the medium is easily assimilated and, therefore, the k value is higher. (Sun et al., 2015).

The GL k-value was higher among the evaluated substrates ($k = 0.168\ d^{-1}$ – Fitzhugh model), indicating its high biodegradability. Among the agro-industrial wastewaters, the highest k-value was obtained for SHW ($k = 0.147\ d^{-1}$ – Fitzhugh model). Therefore, the biomethanization occurred faster than those found for the other substrates, a fact confirmed by the exponential form of its CMPC. According to Wang et al. (2018), SHW has high biodegradability related to soluble compounds, a high concentration of macro and micronutrients, natural buffering, and ready availability of biomolecules that microorganisms can quickly degrade under favorable conditions, which explains the results obtained.

Considering the values estimated by the Fitzhugh model, the lowest speed values were found for DW, BW, and FPW, likely correlated to the change in the CCMP pattern of these substrates, from exponential to sigmoidal shape after the 7th day of the experiment (Fig. 3E, F, and 3G). Intermediate values were observed for RG, SW, and VFA solution.

4. Conclusions

Dairy (DW) and swine (SW) wastewaters, and residual glycerol (RG) from biodiesel production, showed the highest methanization potential, being considered promising substrates to be used in CH_4 producing plants. RG was the substrate that showed the highest biochemical methane potential (BMP).

The methanization kinetics was directly influenced by the substrates' composition and physical-chemical characteristics, which interfere in the anaerobic reactors' mass transfer processes. For these reasons, the methanization of the most particulate wastewaters occurred more slowly and could be expressed by a cumulative methane curve (CMPC) in sigmoidal form. In contrast, the more soluble wastewaters were biodegraded more quickly and presented CMPC in exponential format. In this latter case, exponential kinetic models, especially the Fitzhugh model, could be efficiently applied to describe CH_4 production. However, for complex substrates – with high concentrations of particulate organic matter and oils and greases – logistic kinetic models, such as the Richards and Logistic models, were more reliable and accurate in predicting results.

Declaration of competing interest

The authors declare that they have no known competing financial interests or personal relationships that could have appeared to influence the work reported in this paper.

Acknowledgments

The authors would like to thank the support received from the National Council for Scientific and Technological Development - CNPq, the Coordination for the Improvement of Higher Education Personnel - CAPES, the Minas Gerais State Research Support Foundation - FAPEMIG and the National Institute of Science and Technology in Sustainable Sewage Treatment Stations - INCT Sustainable ETFs.

Appendix A. Supplementary data

Supplementary data to this article can be found online at https://doi.org/10.1016/j.envpol.2021.116876.

Credit author statement

Naassom Wagner Sales Morais: Conceptualization, Investigation, Formal analysis, Writing; **Milena Maciel Holanda Coelho:** Conceptualization, Investigation, Formal analysis, Writing, Amanda de Sousa e Silva: Conceptualization, Investigation, Formal analysis, Writing; **Francisco Schiavon Souza Silva:** Investigation; **Tasso Jorge Tavares Ferreira:** Investigation; **Erlon Lopes Pereira:** Supervision, Conceptualization, Investigation, Formal analysis, Writing; **André Bezerra dos Santos:** Supervision, Conceptualization, Investigation, Formal analysis, Writing.

References

Abu-Reesh, I.M., 2014. Kinetics of anaerobic digestion of labaneh whey in a batch reactor. Afr. J. Biotechnol. 13, 1745–1755. https://doi.org/10.5897/ajb2013.13310.

Afridi, Z.U.R., Wu, J., Li, Z.H., Akand, R., Cao, Z.P., Poncin, S., Li, H.Z., 2018. Novel insight of spatial mass transfer conditions of upflow anaerobic reactor. J. Clean. Prod. 204, 390–398. https://doi.org/10.1016/j.jclepro.2018.09.022.

Ahmadi, E., Yousefzadeh, S., Mokammel, A., Miri, M., Ansari, M., Arfaeinia, H., Badi, M.Y., Ghaffari, H.R., Rezaei, S., Mahvi, A.H., 2020. Kinetic study and performance evaluation of an integrated two-phase fixed-film baffled bioreactor for bioenergy recovery from wastewater and bio-wasted sludge. Renew. Sustain. Energy Rev. 121, 109674. https://doi.org/10.1016/j.rser.2019.109674.

Andriamanohiarisoamanana, F.J., Saikawa, A., Kan, T., Qi, G., Pan, Z., Yamashiro, T., Iwasaki, M., Ihara, I., Nishida, T., Umetsu, K., 2018. Semi-continuous anaerobic co-digestion of dairy manure, meat and bone meal and crude glycerol: process performance and digestate valorization. Renew. Energy 128, 1–8. https://doi.org/10.1016/j.renene.2018.05.056.

Angelidaki, I., Alves, M., Bolzonella, D., Borzacconi, L., Campos, J.L., Guwy, A.J., Kalyuzhnyi, S., Jenicek, P., Van Lier, J.B., 2009. Defining the biomethane potential (BMP) of solid organic wastes and energy crops: a proposed protocol for batch assays. Water Sci. Technol. 59, 927–934. https://doi.org/10.2166/wst.2009.040.

APHA, 2017. – American Public Health Association. Standard Methods for the Examination of Water and Wastewater, 23nd edition. APHA/AWWA/WEF, Washington. 2017.

Aquino, S.F., Chernicharo, C.a.L., Foresti, E., Santos, M.D.L.F., Dos, Monteggia, L.O., 2007. Metodologias para determinação da atividade metanogênica específica (AME) em lodos anaeróbios. Eng. Sanitária Ambient. 12, 192–201. https://doi.org/10.1590/S1413-41522007000200010.

Çetinkaya, A.Y., Yetilmezsoy, K., 2019. Evaluation of anaerobic biodegradability potential and comparative kinetics of different agro-industrial substrates using a new hybrid computational coding scheme. J. Clean. Prod. 238 https://doi.org/10.1016/j.jclepro.2019.117921.

Cheng, D.L., Ngo, H.H., Guo, W.S., Chang, S.W., Nguyen, D.D., Kumar, S.M., Du, B., Wei, Q., Wei, D., 2018. Problematic effects of antibiotics on anaerobic treatment of swine wastewater. Bioresour. Technol. 263, 642–653. https://doi.org/10.1016/j.biortech.2018.05.010.

Coelho, M.M.H., Morais, N.W.S., Pereira, E.L., Leitão, R.C., dos Santos, A.B., 2020. Potential assessment and kinetic modeling of carboxylic acids production using dairy wastewater as substrate. Biochem. Eng. J. 156, 107502. https://doi.org/10.1016/j.bej.2020.107502.

Córdoba, V., Fernández, M., Santalla, E., 2018. The effect of substrate/inoculum ratio on the kinetics of methane production in swine wastewater anaerobic digestion. Environ. Sci. Pollut. Res. 25, 21308–21317. https://doi.org/10.1007/s11356-017-0039-6.

Ding, W., Cheng, S., Yu, L., Huang, H., 2017. Effective swine wastewater treatment by combining microbial fuel cells with flocculation. Chemosphere 182, 567–573. https://doi.org/10.1016/j.chemosphere.2017.05.006.

Dollhofer, V., Dandikas, V., Dorn-In, S., Bauer, C., Lebuhn, M., Bauer, J., 2018. Accelerated biogas production from lignocellulosic biomass after pre-treatment

with Neocallimastix frontalis. Bioresour. Technol. 264, 219–227. https://doi.org/10.1016/j.biortech.2018.05.068.
Donoso-Bravo, A., Pérez-Elvira, S.I., Fdz-Polanco, F., 2010. Application of simplified models for anaerobic biodegradability tests. Evaluation of pre-treatment processes. Chem. Eng. J. 160, 607–614. https://doi.org/10.1016/j.cej.2010.03.082.
Ferreira, D.F., 2019. Sisvar: a computer analysis system to fixed effects split plot type designs. Rev. Bras. Biometria 37, 529–535. https://doi.org/10.28951/rbb.v37i4.450.
Filer, J., Ding, H.H., Chang, S., 2019. Biochemical methane potential (BMP) assay method for anaerobic digestion research. Water (Switzerland) 11. https://doi.org/10.3390/w11050921.
Hammer, Ø., Harper, D.A.T., Ryan, P.D., 2001. PAST: paleontological statistics software package for education and data analysis. Palaeontol. Electron. 4, 1–9.
Holliger, C., Alves, M., Andrade, D., Angelidaki, I., Astals, S., Baier, U., Bougrier, C., Buffière, P., Carballa, M., De Wilde, V., Ebertseder, F., Fernández, B., Ficara, E., Fotidis, I., Frigon, J.C., De Laclos, H.F., Ghasimi, D.S.M., Hack, G., Hartel, M., Heerenklage, J., Horvath, I.S., Jenicek, P., Koch, K., Krautwald, J., Lizasoain, J., Liu, J., Mosberger, L., Nistor, M., Oechsner, H., Oliveira, J.V., Paterson, M., Pauss, A., Pommier, S., Porqueddu, I., Raposo, F., Ribeiro, T., Pfund, F.R., Strömberg, S., Torrijos, M., Van Eekert, M., Van Lier, J., Wedwitschka, H., Wierinck, I., 2016. Towards a standardization of biomethane potential tests. Water Sci. Technol. 74, 2515–2522. https://doi.org/10.2166/wst.2016.336.
Jijai, S., Srisuwan, G., O-thong, S., Norli, I., Siripatana, C., 2016. Effect of substrate and granules/inocula sizes on biochemical methane potential and methane kinetics. Iran. J. Energy Environ. 7, 94–101.
Jiménez-González, C., Woodley, J.M., 2010. Bioprocesses: modeling needs for process evaluation and sustainability assessment. Comput. Chem. Eng. 34, 1009–1017. https://doi.org/10.1016/j.compchemeng.2010.03.010.
Jingura, R.M., Kamusoko, R., 2017. Methods for determination of biomethane potential of feedstocks: a review. Biofuel Res. J. 4, 573–586. https://doi.org/10.18331/BRJ2017.4.2.3.
Kafle, G.K., Chen, L., 2016. Comparison on batch anaerobic digestion of five different livestock manures and prediction of biochemical methane potential (BMP) using different statistical models. Waste Manag. 48, 492–502. https://doi.org/10.1016/j.wasman.2015.10.021.
Kafle, G.K., Kim, S.H., 2012. Evaluation of the biogas productivity potential of fish waste: a lab scale batch study. J. Biosyst. Eng. 37, 302–313. https://doi.org/10.5307/jbe.2012.37.5.302.
Kainthola, J., Shariq, M., Kalamdhad, A.S., Goud, V.V., 2019. Enhanced methane potential of rice straw with microwave assisted pretreatment and its kinetic analysis. J. Environ. Manag. 232, 188–196. https://doi.org/10.1016/j.jenvman.2018.11.052.
Khalid, A., Arshad, M., Anjum, M., Mahmood, T., Dawson, L., 2011. The anaerobic digestion of solid organic waste. Waste Manag. 31, 1737–1744. https://doi.org/10.1016/j.wasman.2011.03.021.
Khan, I.U., Othman, M.H.D., Hashim, H., Matsuura, T., Ismail, A.F., Rezaei-DashtArzhandi, M., Azelee, I.W., 2017. Biogas as a renewable energy fuel – a review of biogas upgrading, utilisation and storage. Energy Convers. Manag. 150, 277–294. https://doi.org/10.1016/j.enconman.2017.08.035.
Kythreotou, N., Florides, G., Tassou, S.A., 2014. A review of simple to scientific models for anaerobic digestion. Renew. Energy 71, 701–714. https://doi.org/10.1016/j.renene.2014.05.055.
Labatut, R.A., Angenent, L.T., Scott, N.R., 2011. Biochemical methane potential and biodegradability of complex organic substrates. Bioresour. Technol. 102, 2255–2264. https://doi.org/10.1016/j.biortech.2010.10.035.
Li, C., Champagne, P., Anderson, B.C., 2011. Evaluating and modeling biogas production from municipal fat, oil, and grease and synthetic kitchen waste in anaerobic co-digestions. Bioresour. Technol. 102, 9471–9480. https://doi.org/10.1016/j.biortech.2011.07.103.
Li, L., Kong, X., Yang, F., Li, D., Yuan, Z., Sun, Y., 2012. Biogas production potential and kinetics of microwave and conventional thermal pretreatment of grass. Appl. Biochem. Biotechnol. 166, 1183–1191. https://doi.org/10.1007/s12010-011-9503-9.
Lier, J.B. van, Zee, F.P. van der, Frijters, C.T.M.J., Ersahin, M.E., 2016. Development of anaerobic high-rate reactors, focusing on sludge bed Technology. In: Hatti-Kaul, R., MGM, B. (Eds.), Anaerobes in Biotechnology. Advances in Biochemical Engineering/Biotechnology. Springer, Cham, pp. 363–395. https://doi.org/10.1007/10.
Lim, S.J., Park, W., Kim, T.H., Shin, I.H., 2012. Swine wastewater treatment using a unique sequence of ion exchange membranes and bioelectrochemical system. Bioresour. Technol. 118, 163–169. https://doi.org/10.1016/j.biortech.2012.05.021.
Lima, D.R.S., Adarme, O.F.H., Baêta, B.E.L., Gurgel, L.V.A., de Aquino, S.F., 2018. Influence of different thermal pretreatments and inoculum selection on the biomethanation of sugarcane bagasse by solid-state anaerobic digestion: a kinetic analysis. Ind. Crop. Prod. 111, 684–693. https://doi.org/10.1016/j.indcrop.2017.11.048.
Lozada, P.T., Vidal, A.P., Cajigas, Á.A., Otero, A.M., González, M., 2008. Selección de acondicionadores químicos para el tratamiento anaerobio de aguas residuales del proceso de extracción de almidón de yuca. Ing. Recur. Nat. y del Ambient 66–74.
Maamri, S., Amrani, M., 2015. Velocity measurement in the steady state is useful to predict the operating conditions for an optimization of thermophilic anaerobic digestion. Int. J. Appl. Microbiol. Biotechnol. Res. 3, 49–61.
Maya-Altamira, L., Baun, A., Angelidaki, I., Schmidt, J.E., 2008. Influence of wastewater characteristics on methane potential in food-processing industry wastewaters. Water Res. 42, 2195–2203. https://doi.org/10.1016/j.watres.2007.11.033.
Mirmohamadsadeghi, S., Karimi, K., Tabatabaei, M., Aghbashlo, M., 2019. Biogas production from food wastes: a review on recent developments and future perspectives. Bioresour. Technol. Reports 7, 100202. https://doi.org/10.1016/j.biteb.2019.100202.
Morais, N.W.S., Coelho, M.M.H., Ferreira, T.J.T., Pereira, E.L., Leitão, R.C., dos Santos, A.B., 2020b. A kinetic study on carboxylic acids production using bovine slaughterhouse wastewater: a promising substrate for resource recovery in biotechnological processes. Bioproc. Biosyst. Eng. https://doi.org/10.1007/s00449-020-02440-3.
Morais, N.W.S., Coelho, M.M.H., Silva, A. de S.e., Pereira, E.L., Leitão, R.C., dos Santos, A.B., 2020a. Kinetic modeling of anaerobic carboxylic acid production from swine wastewater. Bioresour. Technol. 297, 122520. https://doi.org/10.1016/j.biortech.2019.122520.
Mshandete, A., Kivaisi, A., Rubindamayugi, M., Mattiasson, B., 2004. Anaerobic batch co-digestion of sisal pulp and fish wastes. Bioresour. Technol. 95, 19–24. https://doi.org/10.1016/j.biortech.2004.01.011.
O'Melia, C.R., 1980. Aquasols: the behavior of small particles in aquatic systems. Environ. Sci. Technol. 14, 1052–1060. https://doi.org/10.1021/es60169a601.
Pavlostathis, S.G., Giraldo-Gomez, E., 1991. Kinetics of anaerobic treatment: a critical review. Crit. Rev. Environ. Contr. 21, 411–490. https://doi.org/10.1080/10643389109388424.
Pellera, F.M., Gidarakos, E., 2016. Effect of substrate to inoculum ratio and inoculum type on the biochemical methane potential [1] Pellera FM, Gidarakos E. Effect of substrate to inoculum ratio and inoculum type on the biochemical methane potential of solid agroindustrial waste. J Environ. J. Environ. Chem. Eng. 4, 3217–3229. https://doi.org/10.1016/j.jece.2016.05.026.
Pereira, E.L., Borges, A.C., Heleno, F.F., De Oliveira, K.R., Da Silva, G.J., Mounteer, A.H., 2019. Central composite rotatable design for startup optimization of anaerobic sequencing batch reactor treating biodiesel production wastewater. J. Environ. Chem. Eng. 7, 103038. https://doi.org/10.1016/j.jece.2019.103038.
Pereira, E.L., Cristina, T., Paiva, B. De, 2016. Physico-chemical and ecotoxicological characterization of slaughterhouse wastewater resulting from green line. Water, Air, Soil Pollut. https://doi.org/10.1007/s11270-016-2873-4.
Plácido, J., Zhang, Y., 2018. Production of volatile fatty acids from slaughterhouse blood by mixed-culture fermentation. Biomass Convers. Biorefinery 8, 621–634. https://doi.org/10.1007/s13399-018-0313-y.
Rincón, B., Bujalance, L., Fermoso, F.G., Martín, A., Borja, R., 2013. Biochemical methane potential of two-phase olive mill solid waste: influence of thermal pretreatment on the process kinetics. Bioresour. Technol. 140, 249–255. https://doi.org/10.1016/j.biortech.2013.04.090.
Sanjaya, A.P., Cahyanto, M.N., Millati, R., 2016. Mesophilic batch anaerobic digestion from fruit fragments. Renew. Energy 98, 135–141. https://doi.org/10.1016/j.renene.2016.02.059.
Scarlat, N., Dallemand, J.F., Fahl, F., 2018. Biogas: developments and perspectives in europe. Renew. Energy 129, 457–472. https://doi.org/10.1016/j.renene.2018.03.006.
Schneiders, D., Till, A., Lapa, K.R., Pinheiro, A., 2013. Atividade metanogênica específica (AME) de lodos industriais provenientes do tratamento biológico aeróbio e anaeróbio. Rev. Ambient. Água - An Interdiscip. J. Appl. Sci. 8, 135–145. https://doi.org/10.4136/1980-993X.
Silva, A. de S., Morais, N.W.S., Coelho, M.M.H., Pereira, E.L., dos Santos, A.B., 2020. Potentialities of biotechnological recovery of methane, hydrogen and carboxylic acids from agro-industrial wastewaters. Bioresour. Technol. Reports 10, 100406. https://doi.org/10.1016/j.biteb.2020.100406.
Sun, C., Cao, W., Liu, R., 2015. Kinetics of methane production from swine manure and buffalo manure. Appl. Biochem. Biotechnol. 177, 985–995. https://doi.org/10.1007/s12010-015-1792-y.
Turkdogan-Aydinol, F.I., Yetilmezsoy, K., Comez, S., Bayhan, H., 2011. Performance evaluation and kinetic modeling of the start-up of a UASB reactor treating municipal wastewater at low temperature. Bioproc. Biosyst. Eng. 34, 153–162. https://doi.org/10.1007/s00449-010-0456-0.
Wang, S., Hawkins, G.L., Kiepper, B.H., Das, K.C., 2018. Treatment of slaughterhouse blood waste using pilot scale two-stage anaerobic digesters for biogas production. Renew. Energy 126, 552–562. https://doi.org/10.1016/j.renene.2018.03.076.
Ware, A., Power, N., 2017. Modelling methane production kinetics of complex poultry slaughterhouse wastes using sigmoidal growth functions. Renew. Energy 104, 50–59. https://doi.org/10.1016/j.renene.2016.11.045.
Yang, H., Deng, L., Liu, G., Yang, D., Liu, Y., Chen, Z., 2016. A model for methane production in anaerobic digestion of swine wastewater. Water Res. 102, 464–474. https://doi.org/10.1016/j.watres.2016.06.060.
Yao, K.M., Habibian, M.T., O'Melia, C.R., 1971. Water and waste water filtration: concepts and applications. Environ. Sci. Technol. 5, 1105–1112. https://doi.org/10.1021/es60058a005.
Zinatizadeh, A.A., Mohammadi, P., Mirghorayshi, M., Ibrahim, S., Younesi, H., Mohamed, A.R., 2017. An anaerobic hybrid bioreactor of granular and immobilized biomass for anaerobic digestion (AD) and dark fermentation (DF) of palm oil mill effluent: mass transfer evaluation in granular sludge and role of internal packing. Biomass Bioenergy 103, 1–10. https://doi.org/10.1016/j.biombioe.2017.05.006.